*Zootaxa* 5195 (1): 073–086
https://www.mapress.com/zt/


**Article**

ISSN 1175-5326 (print edition)
**ZOOTAXA**
ISSN 1175-5334 (online edition)

https://doi.org/10.11646/zootaxa.5195.1.4
http://zoobank.org/urn:lsid:zoobank.org:pub:15ADF677-471E-4C33-BEA9-ADE6C02CFF4F

# Revised systematic position of *Nasutitermes brevipilus* Emerson, 1925 (Isoptera: Termitidae: Nasutitermitinae) and the designation of *Hyleotermes* gen. nov.

CAROLINA CUEZZO[1], RUDOLF H. SCHEFFRAHN[2*] & REGINALDO CONSTANTINO[3]
[1]*Museu de Zoologia da Universidade de São Paulo, 04263-000 São Paulo, SP, Brazil.*
*carolinacuezzo@gmail.com*
[2]*Fort Lauderdale Research and Education Center, University of Florida, 3205 College Avenue, Davie, Florida 33314, U.S.A.*
*rhsc@ufl.edu; https://orcid.org/0000-0002-6191-5963*
[3]*Departamento de Zoologia, Universidade de Brasília, 70910-900 Brasília, DF, Brazil.*
*constant@unb.br; https://orcid.org/0000-0003-2060-6723*
[*]*Corresponding author*

## Abstract

A new monotypic nasute termite genus, *Hyleotermes* **gen. nov.**, is proposed for *Nasutitermes brevipilus* Emerson, 1925. *Hyleotermes brevipilus*, **comb. nov.**, is redescribed and illustrated based on the morphology of the imago, soldier, and worker castes. It is expanded into Amazonia. The soldier of *Hyleotermes* differs from that of *Nasutitermes* Dudley, 1890 in that the former has a long and cylindrical nasus and the head capsule lacks long setae and is covered with microscopic setae. Unlike the worker of *Nasutitermes*, the *Hyleotermes* worker has a short mixed segment and an enteric valve is adorned with narrow spines on conical bases. The phylogenetic position of *H. brevipilus* comb nov., is reconstructed based on a dataset with two mitochondrial markers (COI and 16SrRNA) for 36 terminals, under maximum likelihood and Bayesian inference. Results corroborate that this species is unrelated to *Nasutitermes* and should be excluded from the genus.

**Key words:** Amazonia, Neotropics, soil-feeder, phylogeny

## Introduction

*Nasutitermes* Dudley, 1890 is the most diverse termite genus with 252 valid species worldwide (Krishna *et al.* 2013, updated). Before 1949, the genus *Nasutitermes* included most termites with nasute soldiers, classified into several subgenera. Snyder (1949) raised all termite subgenera to genus status and later authors further subdivided *Nasutitermes*, describing many new genera. A detailed nomenclatural history for the genus is given in Constantino (2002), Krishna *et al.* (2013), and Boulogne *et al.* (2017).

As evidenced by recent phylogenies (Arab *et al.* 2017; Bourguignon *et al.* 2017), *Nasutitermes* is a heterogeneous assemblage of species, including evolutionary distant lineages from the type-species, *Nasutitermes corniger* (Motschulsky, 1855), not fitting into the current recognized morphological concept of the genus (*sensu* Mathews 1977; Sands 1965, 1998). Particularly, many Neotropical *Nasutitermes* species are in need of complete taxonomic revision, considering especially the worker gut coiling and enteric valve morphology. Roy et al. (2014) lists 16 species from French Guyana that group as *Nasutitermes* s. str.

To reexamine the position of *Nasutitermes brevipilus* Emerson, 1925, we develop a phylogenetic reconstruction based on a dataset with two mitochondrial markers (COI and 16SrRNA) for 36 terminals, under maximum likelihood and Bayesian inference. We describe herein a new monotypic genus, *Hyleotermes* **gen. nov.**, to accommodate *N. brevipilus*, which is redescribed and illustrated based on morphological characters of the imago, soldier and worker castes, and its geographic distribution reaches from Guyana to Amazonian Forest regions of Brazil, Colombia, Ecuador, and Venezuela.

*Accepted by L. Vidlicka: 20 Sept. 2022; published: 10 Oct. 2022*

## Material and methods

**Biological material.** The specimens examined for this study are deposited in the termite collections of the following institutions: American Museum of Natural History, New York, USA (AMNH); Smithsonian National Museum of Natural History, Washington D.C., USA (USNM); University of Florida Termite Collection (UFTC), Fort Lauderdale Research and Education Center, Davie, FL, USA; Departamento de Zoologia, Universidade de Brasília, Brazil (UnB); and Museu de Zoologia da Universidade de São Paulo, SP, Brazil (MZUSP).

**Descriptive terminology and morphometric characters for taxonomic description.** We follow Sands (1998) for the description of the imago-worker mandibles and Noirot (2001) for gut morphology. Terms used for pilosity are comparative. Bristles are long, stiff hairs with well-marked bases. Hairs are shorter and finer than bristles and lack conspicuous bases. Microscopic hairs are visible only under magnification of 40× or higher and with favorable light. Measurements were taken with a micrometric reticle on the eyepiece of a stereoscopic microscope, as follows: length of head with nasus [12]; length of head without nasus [14]; width of head without eyes [18]; diameter of eye [48]; length of ocellus [55]; width of ocellus [56]; eye-ocellus distance [57]; length of pronotum [65]; width of pronotum [68]; length of hind tibia [85]. Numbers in square brackets indicate measurements described in Roonwal (1970). The left mandible index is the ratio between the distance from the apical tooth to the first marginal (M1) and the distance from M1 to M3.

Digital images and drawings. We used a Leica M205C stereomicroscope with dark field illumination to examine the specimens. The enteric valve armature and gizzard of workers were dissected and mounted on microscope slides with Hoyer's medium or glycerol. Imago and worker mandibles were mounted with Euparal. Images were captured with digital cameras attached to a compound light microscope and a stereomicroscope. Depth of field was improved by capturing several images at different focal planes and merging them with CombineZP (Hadley 2010). The distribution map was prepared with Generic Mapping Tools 4.5 (Wessel & Smith 1998).

**Phylogenetic analysis.** The ingroup comprises 34 species of Nasutitermitinae. *Cornitermes cumulans* (Syntermitinae) and *Cylindrotermes parvignathus* (Termitinae) were included as outgroups.

**Molecular characters: DNA extraction, amplification, purification and sequencing.** Genomic DNA was extracted from the head and thorax of soldier/worker specimens preserved in 95% ethanol, with DNeasy Blood & Tissue Kits (Qiagen), following the manufacturer's instructions, and supplemented with 20 mg/ml proteinase K. Abdomens were removed before extraction in order to avoid contaminants from gut contents. The homogenates were incubated at 56 ˚C for 3 h. The COI and 16S markers were then amplified by the polymerase chain reaction (PCR). Primer pairs used to PCR amplification, and also to prime forward and reverse sequencing reactions, were: COI gene (~658 bp), LepF 5-ATTCAACCAATCATAAAGATATTGG-3 and LepR 5-TAAACTTCTGGATGTCCAAAAAATCA-3 (Hajibabaei *et al.* 2006); 16S rRNA gene (~415bp), LR-J-13017: 5-TTACGCTGTTATCCTAA-3 (Kambhampati & Smith 1995) and LR-N-13398 5-CACCTGAACAAAAACAT-3 (Simon *et al.* 1994). COI gene amplifications were performed in 20 μL reactions (10 μL PCR master mix Promega1, 1.5 μM of each primer, 2.5 μL of total DNA, and 6.0 μL deionized water); and 16S gene amplifications in 20 μL reactions (10 μL PCR master mix Promega1, 1.0 μM of each primer, 2.0 μL of total DNA, and 7.0 μL deionized water). PCR was carried out in 40 cycles after initial denaturation at 94 °C for 2 min, denaturation at 94 °C for 1 min, annealing at 43-50 °C (primer pair COI) or 50 °C (primer pair 16S) for 1 min, elongation at 72 °C for 1 min 15 s, and final extension at 72 ˚C for 7 min. Negative controls were run on all amplifications to check for contamination. Amplified PCR products were determined by gel electrophoresis on a 1% agarose gel diluted in TAE buffer (1X) (0.04 M Tris base, 0.02 M acetic acid, and 1 mM EDTA). This same buffer was also used in 1 h electrophoresis runs in an 8-V/cm length gel. All reaction products were purified with ExoSAP (Promega), following the manufacturer's protocols. Purified PCR products were sequenced with the same primers used in the original PCR reactions and the BigDye1 Terminator v3.1 Cycle Sequencing Kit, under the same conditions of PCR. Sequencing was performed in both directions in an ABI Prism DNA sequencer (Applied Biosystems). We visually inspected forward and reverse DNA strands, trimming primers and low-quality ends of sequences, and then assembled them to contigs with Geneious v.9.0.5 (Biomatters Ltd.), under default settings of the MUSCLE alignment algorithm. Some samples for COI were performed at the Canadian Centre for DNA Barcoding following standard high-throughput protocols (deWaard *et al.* 2008). All COI sequences were checked for stop codons and for reading frame shifts by examining translation alignments of the nucleotide data, against the sequence chromatograms. After confirming for no contamination using NCBI BLAST search (http://ncbi.nlm.nih.gov/BLAST), the COI and 16S sequences obtained in this study were combined with

previously published sequences at GenBank (Dietrich & Brune 2016; Bourguignon *et al.* 2017) and the BOLD platform (http://v3.boldsystems.org) to reduce missing information for both, COI and 16S. All sequences were aligned with MAFFT online version (Katoh & Standley 2013), under the FFT-NS-2 (Fast but rough) algorithm (Katoh *et al*. 2002).

**Tree searches**. The phylogenetic analysis applied two model-based methods: maximum likelihood (ML) and Bayesian inference (BI). Prior to analyses, the partition schemes and best-fitting substitution models were selected through the corrected Aikaike Information Criterion (AICc) for four pre-defined data blocks with PartitionFinder2 (Lanfear *et al.* 2016), under a greedy search (Lanfear *et al.* 2012). The data blocks were defined by gene types and by codon positions. The ML analyses were conducted using IQ-TREE v. 1.6.9 (Nguyen *et al.* 2015), and nodal support was estimated with the ultrafast bootstrap method (Hoang *et al.* 2018). The BI was performed with MrBayes 3.2.6 (Ronquist & Huelsenbeck 2003). Two independent runs of four Markov chains (one cold and three hot, with default temperature) each were conducted for 30 million generations, a sampling frequency of one tree every 1000 generations, and a strict consensus tree calculated after discarded the first 25% trees as burn-in. The parameter estimates and convergence of the MCMC output were checked using Tracer v. 1.6.0 (Rambaut *et al.* 2014), ESS values all exceed 200. GenBank accession numbers for all used sequences are available in Table 1.

**TABLE 1.** List of specimens used for phylogenetic reconstruction, with details of sample code, collection locality, and accession numbers.

| Species | Voucher | COI | 16srRNA | **Reference** |
|---|---|---|---|---|
| *Agnathotermes crassinasus* Constantino, 1990 | French Guiana, Petit Saut: G728 | KY224404 | KY224404 | Bourguignon *et al.* 2017 |
| *Agnathotermes glaber* (Snyder, 1926) | Brazil, MG: MZUSP 23746 | MK329282 | MH938368 | Present paper |
| *Anhangatermes macarthuri* Constantino, 1990 | French Guiana, Nouragues: FG-ND2-19 JŠ | KY224556 | KY224556 | Bourguignon *et al.* 2017 |
| *Antillitermes subtilis* (Scheffrahn & Krecek, 1993) | Cuba, Guantanamo: UF CU1184 | MK333228 | N/A | Present paper |
| *Araujotermes caissara* Fontes, 1982 | Brazil, SP: MZUSP 24212 | MK329283 | MH938369 | Present paper |
| *Araujotermes parvellus* (Silvestri, 1923) | French Guiana, Petit Saut: G729 | KY224477 | KY224477 | Bourguignon *et al.* 2017 |
| *Atlantitermes guarinim* Fontes, 1979 | Brazil, SP: MZUSP 24220 | N/A | MH938370 | Present paper |
| *Atlantitermes oculatissimus* (Emerson, 1925) | French Guiana, Petit Saut: G685 | KY224728 | KY224728 | Bourguignon *et al.* 2017 |
| *Caetetermes taquarussu* Fontes, 1981 | French Guiana, Petit Saut: G679 | KP026285 | KP026285 | Bourguignon *et al.* 2015 |
| *Caribitermes discolor* (Banks, 1919) | Dominican Republic, Hispaniola: UF DR139 | MK329284 | N/A | Present paper |
| *Coatitermes clevelandi* (Snyder, 1926) | Brazil, RR: MZUSP 24291 | MK329285 | MH938371 | Present paper |
| *Coatitermes kartaboensis* (Emerson, 1925) | French Guiana, Petit Saut: G740 | KY224708 | KY224708 | Bourguignon et al. 2017 |
| *Coendutermes tucum* Fontes, 1985 | Brazil, RO: MZUSP 19433 | N/A | MH938372 | Present paper |
| *Constrictotermes cyphergaster* (Silvestri, 1901) | Brazil, MG: BRA1 | KY224443 | KY224443 | Bourguignon *et al.* 2017 |
| *Convexitermes manni* (Emerson, 1925) | Paraguay, E Tacuati: UF PA284_01 | MK329286 | N/A | Present paper |

*.....continued on the next page*

**TABLE 1. (Continued)**

| Species | Voucher | COI | 16srRNA | **Reference** |
|---|---|---|---|---|
| *Cornitermes cumulans* (Kollar, 1832) | Brazil, MG: BRA3 | KY224538 | KY224538 | Bourguignon *et al.* 2017 |
| *Cortaritermes silvestrii* (Holmgren, 1910) | Brazil, MG: MZUSP 24727 | N/A | MH938373 | Present paper |
| *Cylindrotermes parvignathus* Emerson, 1949 | French Guiana, Petit Saut: G687 | KY224565 | KY224565 | Bourguignon *et al.* 2017 |
| *Cyranotermes timuassu* Araujo, 1970 | Brazil, MG: MZUSP 24293 | MK329287 | MH938374 | Present paper |
| *Diversitermes diversimiles* (Silvestri, 1901) | Brazil, MS: MZUSP 24512 | MK329288 | N/A | Present paper |
| | Brazil, RO: MZUSP 19460 | N/A | MH938375 | Present paper |
| *Hyleotermes brevipilus* (Emerson, 1925) | Ecuador, Tiputini river: UF EC1165 | MK329289 | N/A | Present paper |
| *Nasutitermes banksi* Emerson, 1925 | French Guiana, Petit Saut: G13-117 | KY224405 | KY224405 | Bourguignon *et al.* 2017 |
| *Nasutitermes corniger* (Motschulsky, 1855) | Guyana | KP091691 | KP091691 | Dietrich & Brune 2016 |
| *Nasutitermes octopilis* Banks, 1918 | French Guiana, Petit Saut: G718 | KY224447 | KY224447 | Bourguignon *et al.* 2017 |
| *Nasutitermes similis* Emerson, 1935 | French Guiana, Petit Saut: G13-127 | KY224557 | KY224557 | Bourguignon *et al.* 2017 |
| *Obtusitermes formosulus* Cuezzo & Cancello, 2009 | Colombia, Puerto Carreno: LS-2015-965 | BOLD: ADK9793 | N/A | http://v3.boldsystems.org |
| *Obtusitermes panamae* (Snyder, 1925) | Panama, Los Piedras: UF_PN1343 | MK329290 | N/A | Present paper |
| *Paraconvexitermes acangapua* Cancello & Noirot, 2003 | Brazil, RO: MZUSP 20335 | N/A | MH938377 | Present paper |
| *Paraconvexitermes junceus* (Emerson, 1949) | Brazil, RR: MZUSP 24303 | MK329291 | MH938376 | Present paper |
| *Parvitermes bacchanalis* Mathews, 1977 | Brazil, MG: MZUSP 23760 | MK329292 | MH938378 | Present paper |
| *Parvitermes brooksi* (Snyder, 1925) | Bahamas, 400 yds S intersec Pirates Way Rd & Great Harbour Dr: UF_BA2949 | MK329293 | N/A | Present paper |
| *Postsubulitermes parviconstrictus* Emerson, 1960 | D.R.Congo, Yangambi: RDCT114 | KY224622 | KY224622 | Bourguignon *et al.* 2017 |
| *Sandsitermes robustus* (Holmgren, 1906) | Peru, 8 km SW von Humbolt: UF_PU751 | MK329294 | N/A | Present paper |
| *Sinqasapatermes sachae* Cuezzo & Nickle, 2011 | Ecuador, Francisco de Orellana: UF_EC1204 | MK329295 | N/A | Present paper |
| *Subulitermes microsoma* (Silvestri, 1903) | Brazil, MG: MZUSP 16252 | MK329296 | N/A | Present paper |
| | Brazil, MS: MZUSP 24298 | N/A | MH938379 | Present paper |
| *Triangularitermes triangulariceps* Mathews, 1977 | Brazil, RO: MZUSP 20463 | MK329297 | MH938380 | Present paper |

## Results and discussion

We assembled a dataset with COI sequences from 17 terminals, which were complemented with other 15 sequences already published in GenBank, plus 16S sequences from 13 terminals, complemented with 15 sequences.

The tree searches results under Bayesian inference (BI, Fig. 1A) and maximum likelihood (ML, Fig. 1B) show high support for the monophyly of the nasutitermitine included. The two approaches also recovered almost the same groups but the lack of resolution at deeper nodes prevented us from answering question about generic relationships. Even though, resultant trees were concordant in recovering *Nasutitermes* species in a relatively high supported single clade, except for *N. brevipilus*, which seems to be related to *Cyranotermes*. We propose herein to create *Hyleotermes* **gen. nov.** to transfer *N. brevipilus* from *Nasutitermes*, by characterizing the new genus with soldier and worker characters.

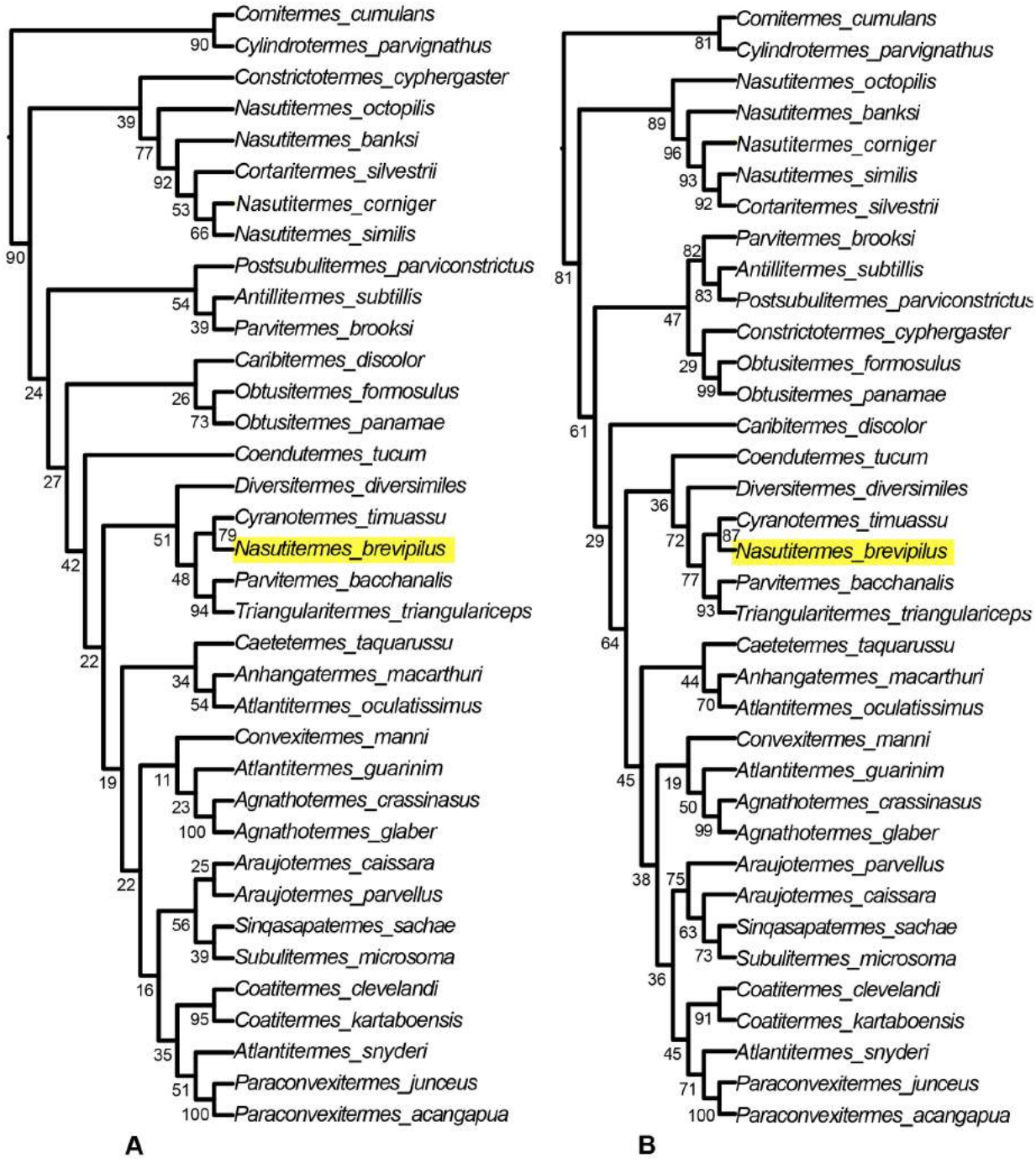


**FIGURE 1.** A, Bayesian inference consensus tree with clade credibility values indicated for each node as percentages; B, Maximum likelihood tree, with ultrafast ML bootstrap values, respectively, labeled at the nodes.

## Taxonomic treatment

### *Hyleotermes* gen. nov.

**Type-species.** *Nasutitermes brevipilus* Emerson, 1925.

**Etymology.** From the Latin word *hylaeus* (Greek *hylaios*), from the forest, meaning a forest termite.

**Included species**. *Hyleotermes brevipilus* (Emerson, 1925)

**Diagnosis.** The head capsule *Hyleotermes* soldier is ovoid in dorsal view, has a long cylindrical nasus, lacks a constriction and long setae, and is covered with microscopic hairs. The mixed segment of the slightly dimorphic worker caste is very short and the enteric valve has six cushions of differing sizes, with each adorned with a few to dozens of narrow spines on conical bases.

**Description**

***Imago***. Eyes large slightly ovoid; ocelli large and elliptical, about as large as antennal socket. Postclypeus slightly arched in profile; midline conspicuous and slightly depressed; anterior margin nearly straight; posterior margin convex. Fontanelle conspicuous, slit-shaped. Epicranial suture faint. Antenna with 15 articles. Mandibular dentition similar to those of worker type 2. Pronotum trapezoidal in dorsal view; anterior and posterior margins nearly rectate. Posterior margin of meso- and metanotum deeply and broadly emarginated; posterolateral corners of meso- and metanotum rounded. Tibial spurs 2:2:2.

***Soldier.*** Monomorphic. In dorsal view, head capsule longer than wide, not constricted. Nasus elongate, subcylindrical. Head capsule, legs, and thoracic sclerites covered with dense short and rather thick hairs. Mandibles with small but well-defined 'points'. Antenna with 12 articles. Postclypeus not convex in profile. Labrum shorter than wide, with rounded anterior margin, parallel lateral margins, and rounded anterior corners. Pronotum with anterior lobe as developed as the posterior one, forming an obtuse angle between them. Procoxa conical, not forming a keel and without a hump on the anterior surface. Tibial spurs 2:2:2.

***Worker.*** Dimorphic, but both types similar in size. Left mandible of type 1 (Fig. 3A) with a narrow gap between the third marginal tooth (M3) and the molar prominence (MP), a darker colored, subtrapezoidal head capsule, and narrower pronotum with its anterior lobe larger than the posterior one. Left mandible of type 2 (Fig. 3B) with a broad gap, a slightly lighter colored head capsule with more convex sides, and a wider pronotum with the anterior lobe about the same size as the posterior one. Both workers with fontanelle situated in the posterior half of the head capsule, pale and slightly depressed, in profile view. Postclypeus not inflated. Antenna with 13 articles. Tibial spurs 2:2:2. Left mandible of both types with apical tooth larger than M1; posterior margin of apical tooth slightly concave; acute angle between posterior margin of apical tooth and anterior margin of M1; posterior margin of M1 sinuous; M3 short but distinct, separated from the molar prominence by a V-shaped gap in worker type I and a broad gap in worker type 2; M4 short, hidden beneath molar prominence; molar prominence concave, with faint ridges. Right mandible with apical tooth larger than M1; M3 reduced, with rounded tip; posterior margin of M3 concave; molar plate concave with faint ridges; basal notch well-defined, but narrow in type 2 workers.

**Gut Coiling** (Figs. 5A–F). Crop slightly more developed than gizzard, partially visible in left lateral view. Mesenteron passing through right side of the abdomen to join the first proctodeal segment (P1) before reaching medial line in ventral view. Very short mixed segment; mesenteric tongue external to the mesenteric arc, not constricted proximally, lateral margins converging distally. Malpighian tubules arranged in two adjacent pairs, but attached on the inner face of the mesenteric arc individually at mesenteron–proctodeum junction; tubules slightly dilated at the attachment point (Fig. 5E). P1 tubular, slightly larger than the mesenteron, reaching left side of abdomen. Distal part of P3 protruding through mesenteric arc, very prominent in dorsal view, notoriously dislocated to left; isthmus conspicuous. Dorsal torsion well developed. 'U-turn' tubular, slightly dilated, visible in lateral right view (Fig. 5F). Distal colon tubular, narrow than the proximal part and joining the rectum in dorsal view.

**Internal compartment ornamentation**. Crop cuticle with pectinate scales. Gizzard (Figs. 6A–C) with completely sclerotized cuticular armature (hexaradial symmetry); pulvillar belt more developed than columnar belt, pulvilli I more developed than pulvilli II, both with their entire surface covered with long aciculiform spines; columns I and II ornamented with short spines. Cuticle of P1 armed with spines only at mesenteron–proctodeum junction. Armature of the enteric valve weakly sclerotized (Fig. 6D), organized in two rings; anterior ring (or upper ring, closest to P1) with 10-20 small spines barely organized in three cushions; posterior ring (or lower ring, closest to P3) with six subconical cushions varying in size; each cushion covered with a few to thirty narrow spines projecting from basal scales (Fig. 7A).

**Comparisons.** The *Hyleotermes brevipilus* soldier is closest to soldiers of *Ereymatermes* Constantino, 1991, and *Subulitermes* Holmgren, 1910 in that all three are small, yellowish in coloration, and have cylindrical nasi. Of these, only the headcapsules of *H. brevipilus*, *S. constricticeps*, Constantino, 1991, and *S. microsoma* (Silvestri, 1903) lack long setae. *Subulitermes constricticeps* and *S. microsoma* are much smaller (mean head width ca. 0.6 mm). The worker enteric valve of *H. brevipilus* is diagnostic and differs those of *Ereymatermes* (Constantino 1991) and *Subulitermes* (Fontes 1986). The following worker characters are distinct in *Nasutitermes* s. str.: EVA with pointed scales on large and small cushions, with trailing columns of scales toward posterior (Fig. 7B); molar plate narrow, straight, with well-developed ridges; each mandible with a short apical tooth and larger marginal teeth; mixed segment very long; enteric valve unsclerotized, with minute spines. Also, in *Nasutitermes* female workers are conspicuously larger than male workers. In all genera of *Nasutitermes* s. str., the worker mandibles have conspicuous molar ridges, and most of them have a long mixed segment.

### *Hyleotermes brevipilus* (Emerson, 1925), comb. nov.

Figs. 2–3, 5–7

*Nasutitermes* (*Nasutitermes*) *brevipilus* Emerson 1925: 395–397 (imago, figs. 63a,b; soldier, figs. 63c,d). *Nasutitermes brevipilus*, Krishna *et al.* 2013: 1660 (catalog)

**Redescription**

***Imago*** (Fig. 2A–C). Head capsule with dense coverage of short fine decumbent hairs and few long scattered erect bristles. Labrum covered by short erect hairs, with two long erect bristles on its midline, and with few shorter bristles at the apex. Pronotum with erect bristles along lateral and posterior margins, and many short fine decumbent hairs over its entire surface. Wing scales with erect bristles, more abundant over costal margin, and with shorter decumbent bristles over entire surface. Meso- and metanotum with many short fine decumbent hairs. Tergites with dense coverage of fine decumbent short bristles, plus row of erect bristles on posterior margin. Sternites with erect bristles over entire surface, plus decumbent ones. Head capsule yellow-brown, with visible lighter frontal marks. Postclypeus yellowish with middle line brown. Labrum pale yellowish. Antennal articles yellow-brown. Legs yellowish. Thoracic nota and tergites yellowish brown; sternites lighter-colored than tergites.

Measurements of two females and five males from sample USNM 2019, range and mean (mm): width of head **without eyes** 0.73–0.77 (0.74), diameter of eye 0.37, length of ocellus 0.13–0.17 (0.15), width of ocellus 0.10–0.13 (0.12), eye-ocellus distance 0.03, width of pronotum 0.83–0.90 (0.86), length of pronotum 0.53–0.60 (0.57), length of hind tibia 1.47–1.53 (1.50).

***Soldier*** (Fig. 2D-E). Head capsule with lateral margins convex, no constriction behind antennal insertion. Dorsal surface of head capsule in profile, converging towards base of nasus with no depression or elevation; vertex outwards in profile. Anterior margin of pronotum rounded, not emarginated. Very short hairs over surface of head capsule, postmentum, legs, and antennae; four short erect bristles on base of nasus; two erect bristles on vertex. Thoracic nota with short hairs over margins. Tergites with decumbent short hairs over surface and a row of four decumbent bristles at posterior margin. Sternites with decumbent short hairs over surface and erect bristles. Head capsule, antenna and postmentum yellowish brown, nasus darker near tip. Thoracic nota, tergites, sternites and legs yellow whitish.

Measurements of 38 soldiers from five samples, range and mean (mm): length of head with nasus 1.56–1.80 (1.68), length of head without nasus 0.88–1.03 (0.95), width of head 0.73–0.90 (0.80), width of pronotum 0.37–0.47 (0.42), length of hind tibia 0.83–1.05 (0.94).

***Worker*** (Figs. 2F-H, 3, 5–6). Head capsule, including postclypeus, with dense coverage of short hairs and eight long erect bristles; postclypeus with two long erect bristles on anterior margin, some short hairs over surface and shorter bristles on posterior margin; pronotum with short hairs on anterior and posterior margins; meso- and metanotum with short hairs; tergites with a row of bristles on posterior margin and many hairs over surface.

Measurements of workers from four colonies, range and mean (mm); see Fig. 4 for morphometric differences between the two worker types. Type 1 (n = 25): width of head 0.68–0.77 (0.72), width of pronotum 0.38–0.43 (0.40), length of hind tibia 0.70–0.87 (0.79); Type 2 (n = 19): width of head 0.67–0.77 (0.74), width of pronotum 0.44–0.48 (0.46), length of hind tibia 0.80–0.95 (0.89). Left mandible index (n = 23): 0.70.

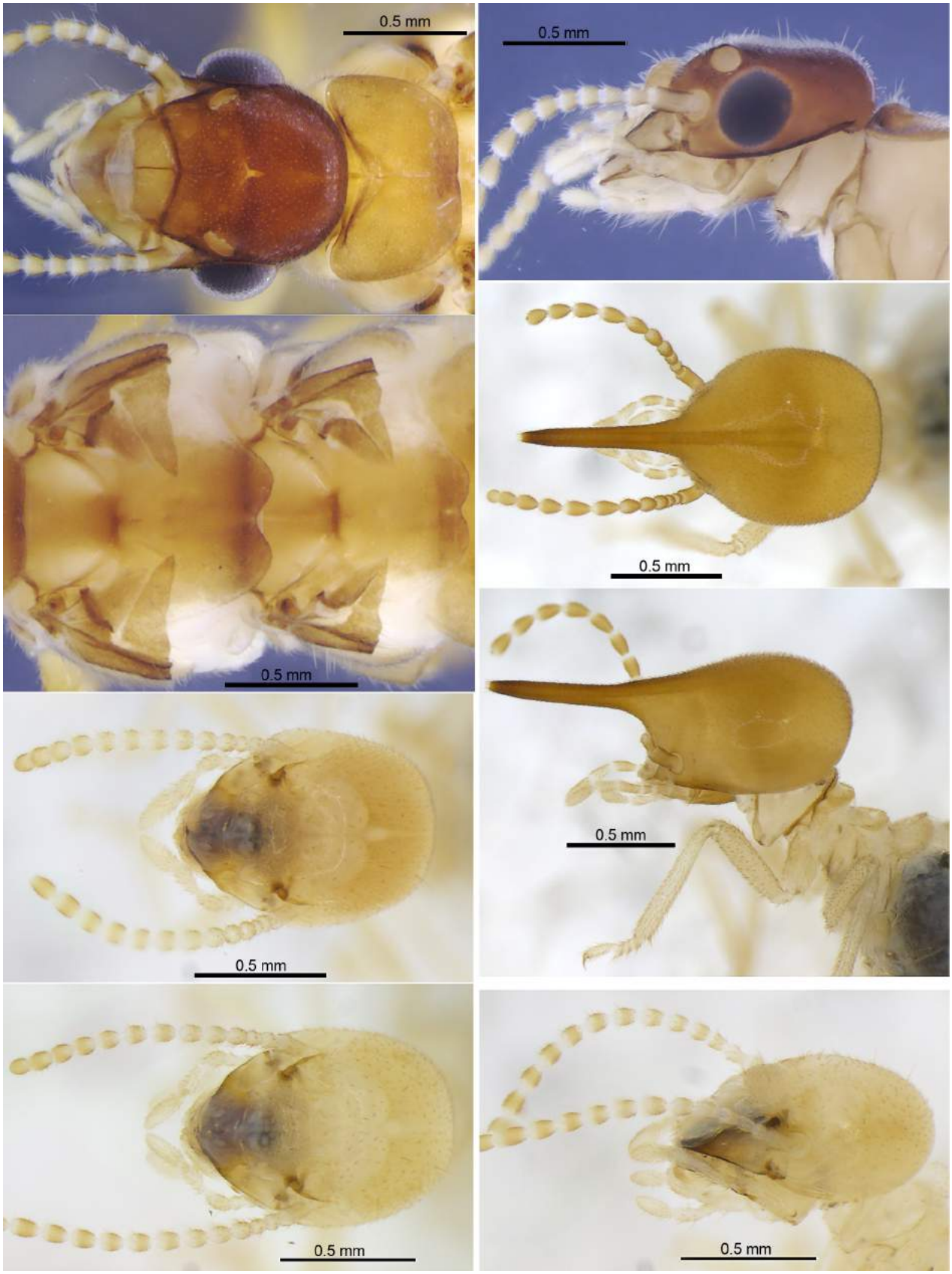


**FIGURE 2.** Imago, soldier, and workers of *Hyleotermes brevipilus*, **comb. nov.** A, head and pronotum of female imago (paratype) in dorsal view; B, head of imago in profile; C, meso and metanotum of imago in dorsal view; D, soldier head in profile; E, soldier head in dorsal view; F, worker type 1 (narrow gap), head in dorsal view; G, worker type 2 (broad gap), head in dorsal view; H, worker type 2 (broad gap), head in profile view.

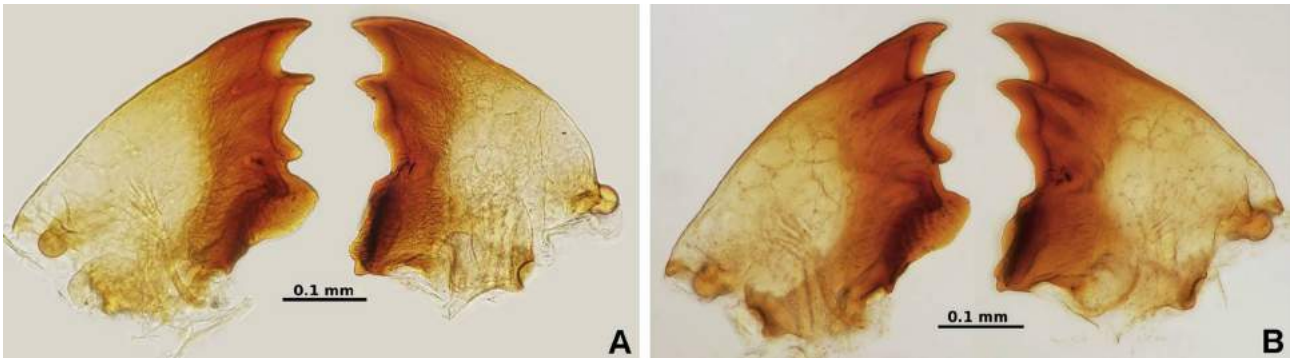


**FIGURE 3.** Worker mandibles of *Hyleotermes brevipilus*, **comb. nov.** A, type 1 (narrow gap); B, type 2 (broad gap). Gap is between the third marginal tooth (M3) and molar prominence (MP) of left mandibles.

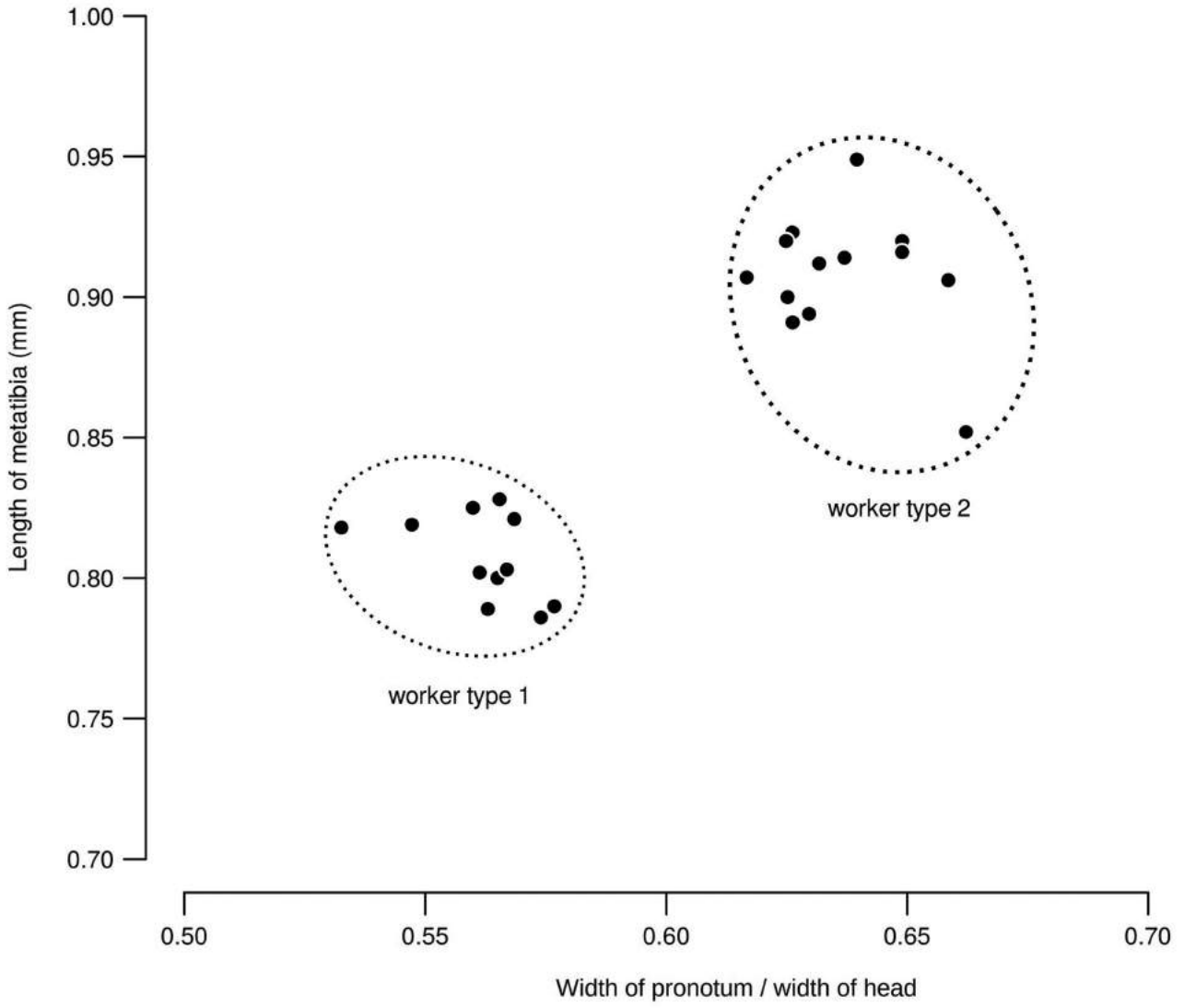


**FIGURE 4.** Scatterplot showing morphometric differences between the two worker types of *Hyleotermes brevipilus*, **comb. nov.**

**Distribution** (Fig. 7). Amazon region of Brazil, Colombia, Ecuador, Guyana, and Venezuela.

**Material examined.** ***Type material***: Holotype: female imago, Guyana, Bartica District, Kartabo (6.38N 58.7W), 16.viii.1920, A. E. Emerson coll. and det., AMNH, #214. Paratypes: same data sample as holotype, imagos, soldiers (including a "morphotype"), and workers (AMNH); and another sample from the same locality, 19.vii.1920, A. E. Emerson coll. and det., imagos, soldiers, workers, larvae and presoldier (USNM-2019). ***Other material***: BRAZIL.

*State of Amazonas*. São Gabriel da Cachoeira (0.13S 67.089W): soldiers, workers, 15.x.2007, D.R.M. Mendonça leg. (UnB-7613). *State of Mato Grosso*. Juruena: Rohden Lignea (10.469S 58.582W): soldiers, workers, 03.vii.2002, R. Constantino leg. (UnB-3334). COLOMBIA. *Caquetá*. San Vicente del Caguan (2.114N 74.769W): soldiers and workers, 19.iv.2018, Daniel Castro leg. (UFTC-CO914). ECUADOR. *Orellana Province*. Tiputini River (0.675S 76.369W): soldiers, workers, 01.vi.2011, R.H. Scheffrahn leg. (UFTC-EC1165). VENEZUELA. *State of Bolívar*. La Culebra—Auyantepui (6.683N 66.967W): soldiers, workers, 24.i.1991, C.J. Rosales leg. (UnB-2014).

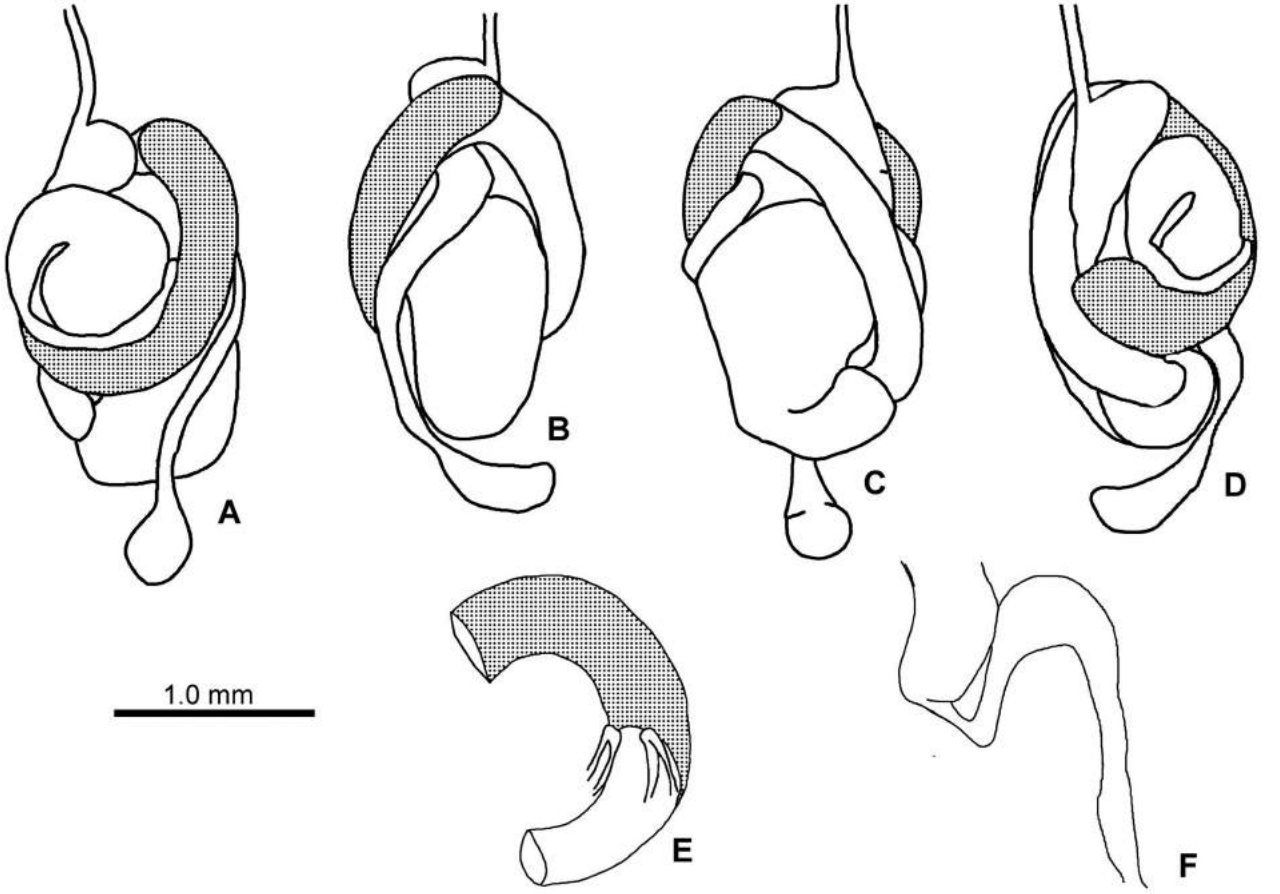


**FIGURE 5.** Gut morphology of the worker of *Hyleotermes brevipilus*, **comb. nov.** gut *in situ*; A, dorsal; B, left; C, ventral; D, right; E, mixed segment and attachment of Malpighian tubes; F, segment of proctodeum (P3–P4) showing the isthmus.

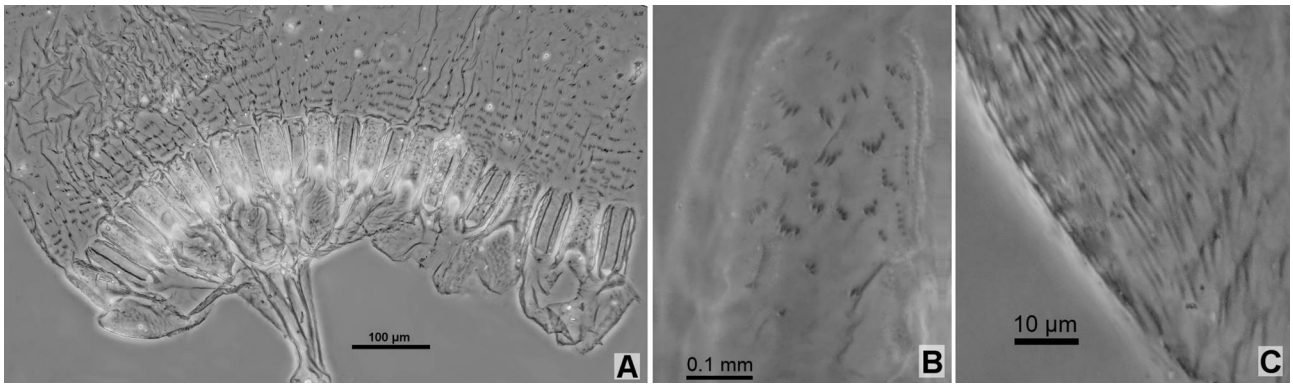


**FIGURE 6.** Gizzard and enteric valve of the worker of *Hyleotermes brevipilus*, **comb. nov.** A, complete gizzard armature, showing columnar and pulvillar belts; B, detail of column I, ornamented with scales; C, detail of pulvillus I with their entire surface covered with long aciculiform spines.

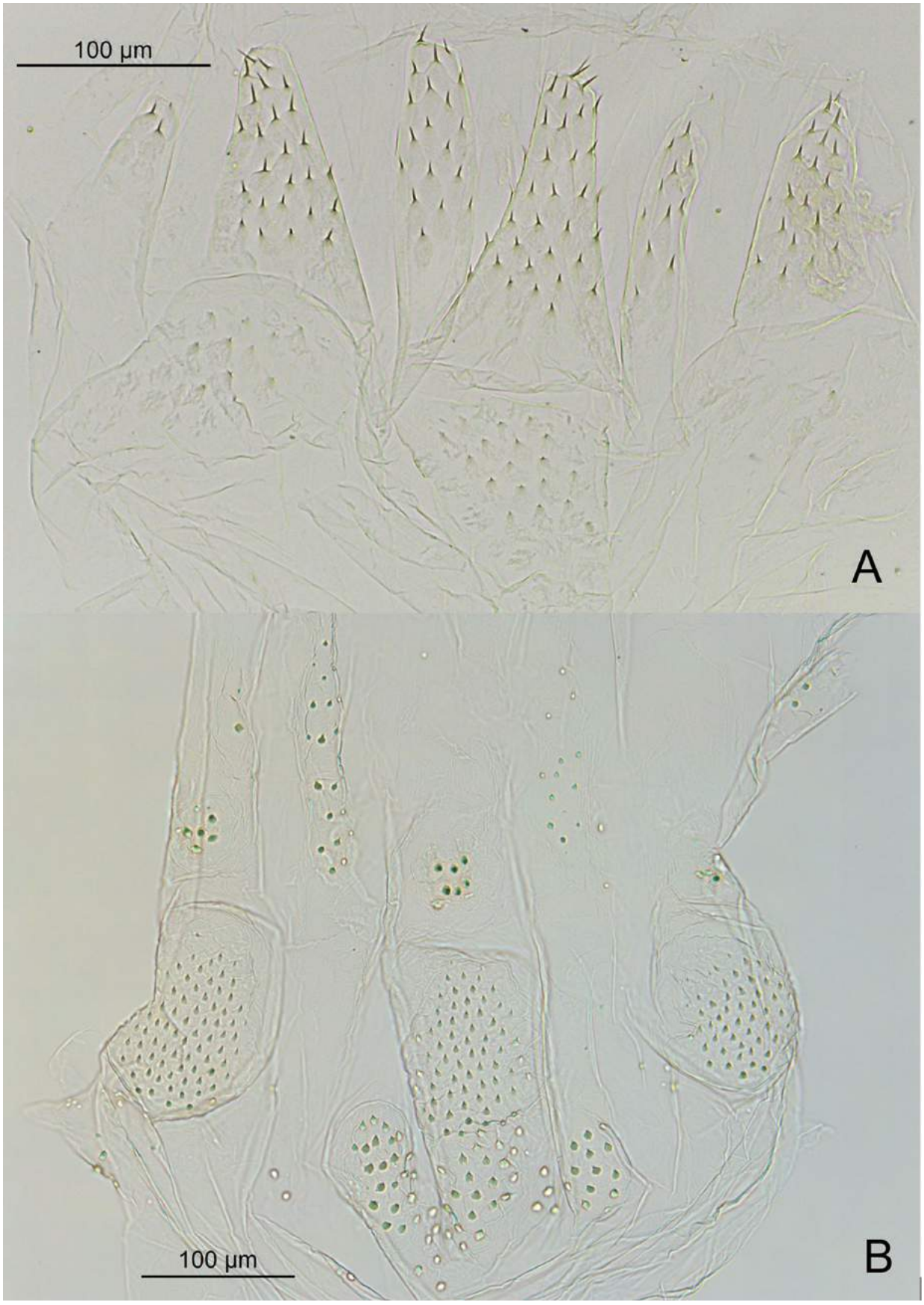


**FIGURE 7.** Worker enteric valve armature of A, *Hyleotermes brevipilus* **comb. nov.**; B, *Nasutermes corniger* from Panama (UFTC no. PN379).

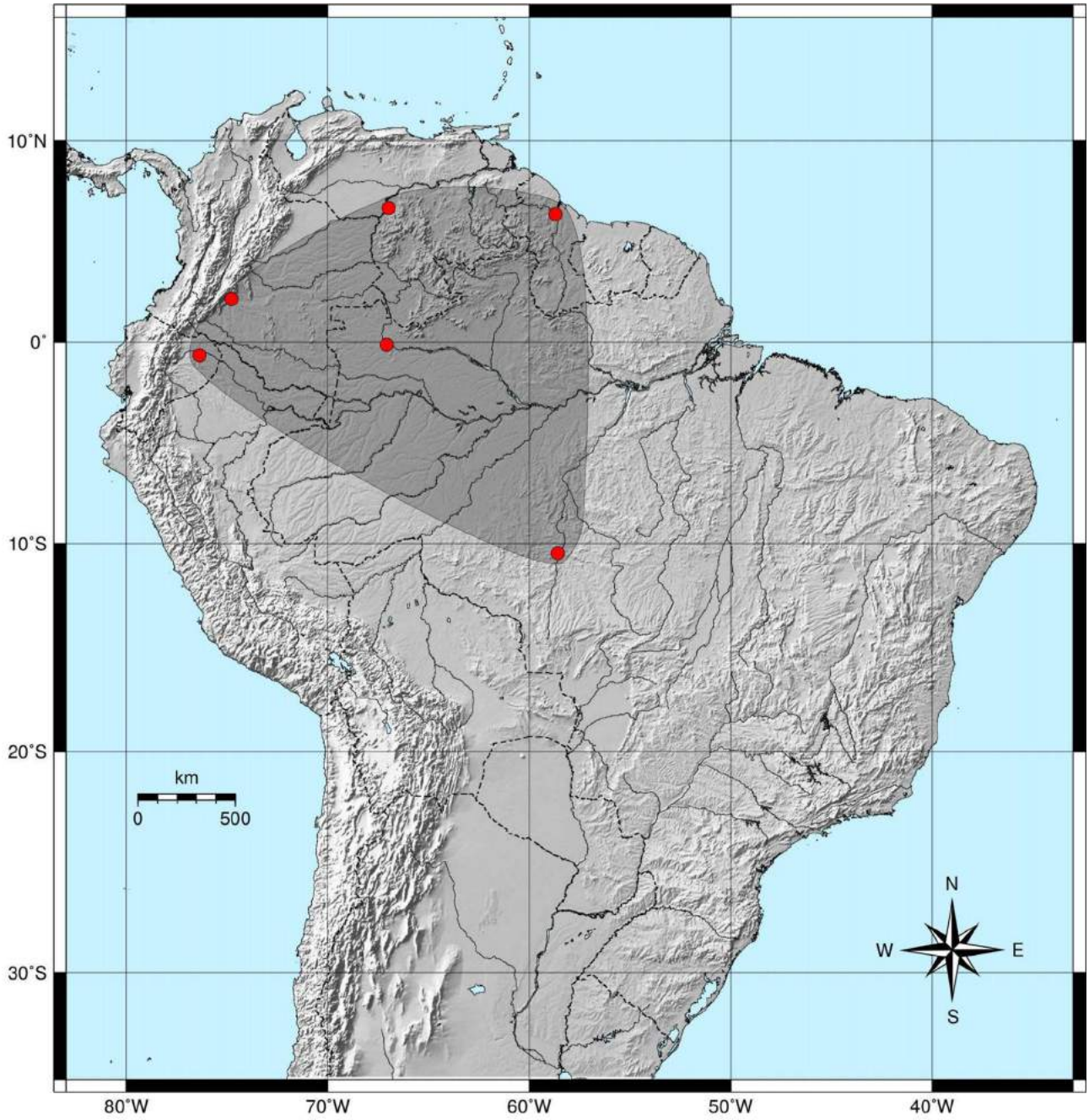


**FIGURE 8.** Geographic distribution of *Hyleotermes brevipilus*, **comb. nov.**


## Acknowledgments

We thank Kumar Krishna and David Grimaldi for assistance during visits to the AMNH, and David Nickle during a visit to the USNM; *Jaqueline Battilana* and Maria Augusta Ribeiro **support** from MZUSP Biomol Lab. Carolina Cuezzo received financial support from the São Paulo Research Foundation, Brazil (FAPESP grant 2013/05610-1), and R. Constantino was supported by Brazilian National Research Council (CNPq grants 481360/2013-1 and 306815/2013-3).

## References


Arab, D.A., Namyatova, A., Evans, T.A., Cameron, S.L., Yeates, D.K., Ho, S.Y. & Lo, N. (2017) Parallel evolution of mound-building and grass-feeding in Australian nasute termites. *Biology Letters*, 13, 20160665. https://doi.org/10.1098/rsbl.2016.0665

Bourguignon, T., Lo, N., Šobotník, J., Ho, S.Y.W., Iqbal, N., Coissac, E., Lee, M., Jendryka, M.M., Sillam-Dussès, D., Křížková, B., Roisin, Y. & Evans T.A. (2017) Mitochondrial phylogenomics resolves the global spread of higher termites, ecosystem engineers of the tropics. *Molecular Biology and Evolution*, 34, 589–597. https://doi.org/10.1093/molbev/msw253

Boulogne, I., Constantino, R., Amusant, N., Falkowski, M., Rodrigues, A.M.S. & Houël, E. (2017) Ecology of termites from the genus *Nasutitermes* (Termitidae: Nasutitermitinae) and potential for science-based development of sustainable pest management programs. *Journal of Pest Science*, 90, 19–37. https://doi.org/10.1007/s10340-016-0796-x

Constantino, R. (1991) *Ereymatermes rotundiceps*, new genus and species of termite from the Amazon Basin (Isoptera, Termitidae, Nasutitermitidae). *Goeldiana Zoologia*, 8, 1–11.

Constantino, R. (2002) Notes on the type-species and synonymy of the genus *Nasutitermes* (Isoptera: Termitidae: Nasutitermitinae). *Sociobiology*, 40, 533–537.

Dietrich, C. & Brune, A. (2016) The complete mitogenomes of six higher termite species reconstructed from metagenomic datasets (*Cornitermes* sp., *Cubitermes ugandensis*, *Microcerotermes parvus*, *Nasutitermes corniger*, *Neocapritermes taracua*, and *Termes hospes*). *Mitochondrial DNA*, Part A, 27, 3903–3904. https://doi.org/10.3109/19401736.2014.987257

Emerson, A.E. (1925) The termites from Kartabo, Bartica District, Guyana. *Zoologica*, 6, 291–459. https://doi.org/10.5962/p.190324

Fontes, L.R. (1986) Morphology of the worker digestive tube of the soil-feeding nasute termites (Isoptera, Termitidae, Nasutitermitinae) from the Neotropical region. *Revista brasileira de Zoologia*, 3, 475–501. https://doi.org/10.1590/S0101-81751986000400002

Hadley, A. (2010) CombineZP. Software. Available from: http://www.hadleyweb.pwp.blueyonder.co.uk (accessed 22 September 2022)

Hajibabaei, M., Janzen, D.H., Burns, J.M., Hallwachs, W. & Hebert, P.D. (2006) DNA barcodes distinguish species of tropical Lepidoptera. *Proceedings of the National Academy of Sciences*, 103, 968–971. https://doi.org/10.1073/pnas.0510466103

Hoang, D.T., Chernomor, O., Haeseler, A. von, Minh, B.Q. & Vinh, L.S. (2018) UFBoot2: Improving the Ultrafast Bootstrap Approximation. *Molecular Biology and Evolution*, 35, 518–522. https://doi.org/10.1093/molbev/msx281

Kambhampati, S. & Smith, P.T. (1995) PCR primers for the amplification of four insect mitochondrial gene fragments. *Insect Molecular Biology*, 4, 233–236. https://doi.org/10.1111/j.1365-2583.1995.tb00028.x

Katoh, K. & Standley, D.M. (2013) MAFFT multiple sequence alignment software version 7: improvements in performance and usability. *Molecular Biology and Evolution*, 30, 772–780. https://doi.org/10.1093/molbev/mst010

Katoh, K., Misawa, K., Kuma, K. & Miyata, T. (2002) MAFFT: a novel method for rapid multiple sequence alignment based on fast Fourier transform. *Nucleic Acids Research*, 30, 3059–3066. https://doi.org/10.1093/nar/gkf436

Krishna, K., Grimaldi, D.A., Krishna, V. & Engel, M.S. (2013) Treatise on the Isoptera of the world. *Bulletin of the American Museum of Natural History*, 377, 1–2704.
https://doi.org/10.1206/377.1
https://doi.org/10.1206/377.2
https://doi.org/10.1206/377.3
https://doi.org/10.1206/377.4
https://doi.org/10.1206/377.5
https://doi.org/10.1206/377.6
https://doi.org/10.1206/377.7

Lanfear, R., Calcott, B., Ho, S.Y. & Guindon, S. (2012) PartitionFinder: combined selection of partitioning schemes and substitution models for phylogenetic analyses. *Molecular Biology and Evolution*, 29, 1695–1701. https://doi.org/10.1093/molbev/mss020

Lanfear, R., Frandsen, P.B., Wright, A.M., Senfeld, T. & Calcott, B. (2016) PartitionFinder 2: new methods for selecting partitioned models of evolution for molecular and morphological phylogenetic analyses. *Molecular Biology and Evolution*, 34, 772–773. https://doi.org/10.1093/molbev/msw260

Mathews, A.G.A. (1977) *Studies on Termites from Mato Grosso State, Brazil*. Academia Brasileira de Ciências, Rio de Janeiro, 267 pp.

Nguyen, L.-T., Schmidt, H.A., von Haeseler, A. & Minh, B.Q. (2015) IQ-TREE: A fast and effective stochastic algorithm for estimating maximum-likelihood phylogenies. *Molecular Biology and Evolution,* 32, 268–274. https://doi.org/10.1093/molbev/msu300

Noirot, C. (2001) The gut of termites (Isoptera). Comparative anatomy, systematics, phylogeny. I. Higher termites (Termitidae). *Annales de la Société Entomologique de France*, 37, 431–471.

Rambaut, A., Suchard, M.A, Xie, D. & Drummond, A.J. (2014) Tracer. Version 1.6. Available from: http://beast.bio.ed.ac.uk/Tracer (accessed 22 September 2022)

Ronquist, F. & Huelsenbeck, J.P. (2003) MrBayes 3: Bayesian phylogenetic inference under mixed models. *Bioinformatics*, 19, 1572–1574.

Roonwal, M.L. (1970) Measurement of termites (Isoptera) for taxonomic purposes. *Journal of the Zoological Society of India*, 21, 9–66.

Roy, V., Constantino, R., Chassany, V., Giusti-Miller, S., Diouf, M., Mora, P. & Harry, M. (2014) Species delimitation and phylogeny in the genus *Nasutitermes* (Termitidae: Nasutitermitinae) in French Guiana. *Molecular Ecology*, 23, 902–920. https://doi.org/10.1111/mec.12641

Sands, W.A. (1965) A revision of the termite subfamily Nasutitermitinae (Isoptera, Termitidae) from the Ethiopian region. *Bulletin of the British Museum (Natural History), Entomology*, 4, 1–172.

Sands, W.A. (1998) *The identification of worker castes of termite genera from soils of Africa and the Middle East*. Cab International, Wallingford, 475 pp., 18 pls.

Simon, C., Frati, F., Beckenbach, A., Crespi, B., Liu, H. & Flook, P. (1994) Evolution, weighting and phylogenetic utility of mitochondrial gene sequences and a compilation of conserved polymerase chain reaction primers. *Annals of the Entomological Society of America*, 87, 651–701. https://doi.org/10.1093/aesa/87.6.651

Snyder, T.E. (1949) Catalog of the termites (Isoptera) of the World. *Smithsonian Miscellaneous Collections*, 112, 1–490.

deWaard, J.R., Ivanova, N.V., Hajibabaei, M. & Hebert, P.D.N. (2008) Assembling DNA Barcodes: Analytical Protocols. *In*: Cristofre, M.C. (Ed.), *Methods in Molecular Biology 410: Environmental Genetics*. Humana Press, Totowa, New Jersey, pp. 275–293. https://doi.org/10.1007/978-1-59745-548-0_15

Wessel, P. & Smith, W.H.F. (1998) New, improved version of Generic Mapping Tools released. *EOS, Transactions of the American Geophysical Union*, 79, 579. https://doi.org/10.1029/98EO00426